AIP | Journal of Applied Physics

Impact of incomplete ionization of dopants on the electrical properties of compensated p-type silicon

M. Forster, A. Cuevas, E. Fourmond, F. E. Rougieux, and M. Lemiti

Citation: J. Appl. Phys. **111**, 043701 (2012); doi: 10.1063/1.3686151
View online: http://dx.doi.org/10.1063/1.3686151
View Table of Contents: http://jap.aip.org/resource/1/JAPIAU/v111/i4
Published by the American Institute of Physics.

Impact of incomplete ionization of dopants on the electrical properties of compensated *p*-type silicon

M. Forster,[1,2,3,a)] A. Cuevas,[2] E. Fourmond,[3] F. E. Rougieux,[2] and M. Lemiti[3]
[1]*APOLLON SOLAR, 66 cours Charlemagne, 69002 Lyon, France*
[2]*School of Engineering, College of Engineering and Computer Science, The Australian National University, Canberra ACT 0200, Australia*
[3]*INSA de LYON, INL, 7 av. J. Capelle, 69621 Villeurbanne Cedex, France*

(Received 18 October 2011; accepted 18 January 2012; published online 17 February 2012)

This paper investigates the importance of incomplete ionization of dopants in compensated *p*-type Si and its impact on the majority-carrier density and mobility and thus on the resistivity. Both theoretical calculations and temperature-dependent Hall-effect measurements demonstrate that the carrier density is more strongly affected by incomplete ionization in compensated Si than in uncompensated Si with the same net doping. The previously suggested existence of a compensation-specific scattering mechanism to explain the reduction of mobility in compensated Si is shown not to be consistent with the *T*-dependence of the measured carrier mobility. The experiment also shows that, in the vicinity of 300 K, the resistivity of compensated Si has a much weaker dependence on temperature than that of uncompensated silicon. © *2012 American Institute of Physics*. [doi:10.1063/1.3686151]

I. INTRODUCTION

The equilibrium carrier density (p_0) in the base of crystalline silicon (Si) solar cell devices has a great influence on their performance. Especially in boron (B) and phosphorus (P) compensated Si, such as low-cost upgraded metallurgical-grade (UMG) Si,[1] p_0 has been found both by theoretical[2,3] and experimental studies[2,4–7] to be a key parameter to optimize the material's electrical properties and the device performance. Most of the recently published papers[3,6,8–11] dealing with compensated Si consider p_0 to be equal to the net doping N_A-N_D, implicitly assuming that all the dopants are ionized at room temperature (T). While neglecting incomplete ionization (i.i.) is usually a fair assumption for devices made of uncompensated electronic-grade (EG)-Si with relatively low doping ($\sim 10^{16}$ cm^{-3}), it becomes questionable for the higher dopant concentrations that might be encountered in compensated UMG-Si. In addition, the usage of gallium (Ga) as a third compensating dopant was recently proposed to overcome net doping variations during crystallization of B and P compensated Si feedstock.[5,12] In that case, due to the higher ionization energy of Ga in Si compared to B, it is necessary to treat the matter of i.i. with even more attention.

In this work, we aim at assessing the impact of i.i. on the equilibrium carrier density in compensated Si. We show, through both theoretical calculations and experimental investigation using *T*-dependent Hall effect measurements, that room-*T* i.i. is more important in compensated Si and that it must be considered to evaluate p_0 whenever the Si contains more than 5×10^{16} cm^{-3} of B or 2×10^{16} cm^{-3} of Ga.

Majority-carrier mobility (μ_h) reduction was previously observed[10,12–15] in compensated Si and was shown not to be described by standard mobility models. An understanding of the physical mechanism responsible for this reduction is necessary to improve the models in order to predict the mobility with a greater accuracy in compensated Si. Previous studies attribute it either to the existence of a compensation-specific scattering mechanism[13,15] or to the reduction of ionized impurities screening by free carriers in compensated Si.[14] Through a thorough analysis of the *T*-dependence of μ_h and using incomplete ionization as a mean to tune the compensation level, we show that neither of these two explanations is consistent with experimental results.

In the last section of the paper, we finally discuss how the *T*-dependences of p_0 and μ_h lead to a more stable resistivity ρ in highly-doped compensated Si around room-*T*.

II. METHODS

A. Calculating incomplete ionization

The ionization of a dopant located in a substitutional position of the Si lattice is governed by the occupancy of its energy ground state. Under equilibrium, this occupancy depends on the position of the Fermi energy level (E_F) with respect to the dopant energy level (E_A), according to the Fermi-Dirac statistics Eq. (1):

$$\frac{N_A^-}{N_A} = \frac{1}{1 + g \cdot \exp\left(\frac{E_A - E_F}{kT}\right)}. \quad (1)$$

Since each acceptor level is able to accept one hole of either spin together with the fact that there are two degenerate valence bands, acceptor ground states in Si are fourfold degenerate and the degeneracy factor g used in Eq. (1) is therefore taken as equal to 4.[16] The equilibrium electron and hole densities n_0 and p_0 can be expressed in a simple manner as a function of E_F using Boltzmann statistics [Eqs. (2) and (3)] which applies to non-degenerate semiconductors considered in this work. In Eqs. (2) and (3), the effective densities of states N_C and N_V, respectively in the conduction and in the

a)Electronic mail: maxime.forster@insa-lyon.fr.

valence band are calculated using the parameterization given in Ref. 17.

$$n_0 = N_C \exp\left(-\frac{E_C - E_F}{kT}\right), \quad (2)$$

$$p_0 = N_V \exp\left(-\frac{E_F - E_V}{kT}\right). \quad (3)$$

By numerically solving the Poisson equation, which simplifies to

$$p_0 + \sum N_D = n_0 + \sum N_A^-, \quad (4)$$

in the case of uniform bulk doping, we determine the only E_F that allows the neutrality condition to be satisfied[16] and deduce all the relevant parameters to study i.i. Since we only consider the case of *p*-type Si, E_F is systematically in the lower half of the bandgap and thus far below the energy level of donor dopants such as phosphorus. Donor dopants are therefore completely ionized in compensated *p*-type Si and remain so even at very low *T*.

E_A varies with dopant concentration as the metal−nonmetal (MNM) transition is approached. The mechanisms occurring near the MNM transition have been well explained by Altermatt *et al*. who derived a parameterization for most commonly used dopants.[18,19] In the present work, we use this parameterization Eq. (5), whose constants $E_{A,0}$, N_{ref}, and *c* are reported in Table I, to account for the variation of the energy level of B (Fig. 1). Since no parameterization was found in the literature for Ga-doping, we use a fit of Eq. (5) to experimental data[20,21] on Ga-doped Si (Fig. 1). Constants used for this fit are also given in Table I. By using this parameterization, we assume E_A not to be affected by compensation. The validity of this assumption will be discussed later in this paper by contrasting calculations to experimental data. It is also worth noting that this parameterization may not be valid for gallium concentrations higher than 3×10^{18} cm^{-3} for which there are no experimental data available. For that reason, we represent E_A above 3×10^{18} cm^{-3} with a dotted line, to indicate that our parameterization is likely not to be valid in this concentration range.

$$E_A = \frac{E_{A,0}}{1 + (N_A/N_{ref})^c}. \quad (5)$$

This method to calculate i.i. is substantially the same as that recently presented in Ref. 7, apart from the fact that we do not neglect the minority-carrier density when solving the Poisson equation. This allows for extending the calculation to a broader range of *T* if needed, like when modeling the carrier density near or in the intrinsic range, for example during ingot cooling or high temperature cell processing steps.

TABLE I. Constants used for the calculation of E_A for B and Ga.

Dopant	$E_{A,0}$ (meV)	N_{ref} (cm^{-3})	*c*
B	44.4	1.3×10^{18}	1.4
Ga	72.0	5.0×10^{18}	0.75

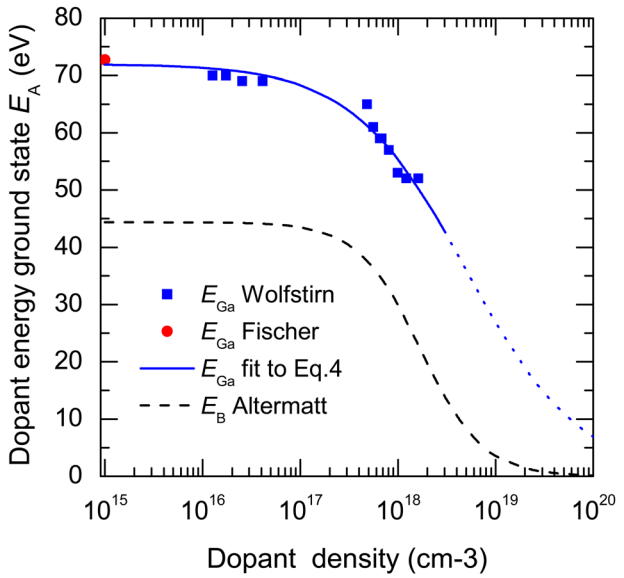

FIG. 1. (Color online) Evolution of the activation energy of B and Ga as a function of dopant concentration.

B. Experimental details

To study the *T*-dependence of the carrier density, we have carried out Hall-effect measurements with an Ecopia HMS-5000 device equipped with a liquid nitrogen temperature control system. The resistivity ρ and the Hall carrier density p_H were measured on a Van Der Pauw configuration on 2×2 cm^2 square Si samples between 80 and 350 K. Good ohmic contacts were achieved by using indium-gallium eutectic alloy. The actual carrier density p_0 was then calculated from the measured p_H with Eq. (6) using the *T*-dependent Hall factor r_H as calculated by Szmulowicz.[22] By doing so, we assume r_H not to be affected by compensation, which has been revealed to be the case at room-*T* in three independent studies.[10,13,15]

$$p_0 = r_H \cdot p_H. \quad (6)$$

Measurements were done on a B-doped sample (sample B-1) and on another sample co-doped with B, P, and Ga (sample C-1) of similar N_A-N_D. Both samples were cut from a 125×125 cm^2 wafer which originate from <100>-oriented Czochralski (Cz)-grown Si ingots. The B concentration in sample B-1 was deduced from 4-point probe resistivity measurement to be 0.9×10^{16} cm^{-3}. The dopants concentrations in the co-doped sample were estimated from its position in the originating ingot using Scheil's segregation law. All dopants concentrations are reported in Table II. The data obtained on these two samples are compared throughout the rest of the paper to Hall data reported by Hoshikawa *et al*.[23] measured on Ga-doped Cz-Si of similar doping density (sample G-1).

III. RESULTS AND DISCUSSION

A. Incomplete ionization and carrier density

To consider i.i. in compensated *p*-type Si, one can either look at the fraction of ionized acceptors N_A^-/N_A or at the

TABLE II. Dopants concentrations in all three samples investigated in this work.

Sample	B (cm^{-3})	Ga (cm^{-3})	P (cm^{-3})	N_A-N_D (cm^{-3})
B-1	0.9×10^{16}	…	…	0.9×10^{16}
C-1	2.2×10^{16}	5.7×10^{16}	7.1×10^{16}	0.8×10^{16}
G-1	…	1.0×10^{16}	…	1.0×10^{16}

ratio of the carrier density to the net doping $p_0/(N_A\text{-}N_D)$. Unlike in uncompensated Si, these two ratios differ in compensated Si. In this section, we intend to assess the impact of i.i. on p_0 which, as mentioned above, has a great influence on the electrical properties of Si materials and solar cells. For that purpose, the most relevant parameter to focus on in order to assess the impact of i.i. and the error that is made when neglecting it (i.e., assuming $p_0 = N_A\text{-}N_D$) is therefore $p_0/(N_A\text{-}N_D)$. This ratio is referred to in the rest of the paper as the i.i. ratio.

We also define the compensation level C_l, which is meant to represent how close to each others the acceptor and the donor concentrations are. To calculate C_l, one can either use the ionized or the total dopant concentrations. From a physical point of view, it is more meaningful to use the ionized dopant concentrations, as is done in Eq. (7), since neutral impurities do not affect the electrical properties of Si:

$$C_l = \frac{N_A^- + N_D^+}{N_A^- - N_D^+} \approx \frac{N_A^- + N_D^+}{p_0}. \quad (7)$$

However, for more simplicity, we will use in the following section (Sec. III A 1) C_l as calculated with the total dopant concentrations [$C_l = (N_A + N_D)/(N_A - N_D)$]. Bearing in mind that it is not meaningful in terms of electrical properties, it is meant to give an insight of the effect of adding compensating P atoms on the importance of room-T incomplete ionization on p_0.

1. Room-temperature incomplete ionization

Figure 2 shows the result of our calculations at 300 K for [B] ranging from 1×10^{16} cm^{-3} to 5×10^{17} cm^{-3} compensated with various amounts of P. In uncompensated Si ($C_l = 1$), E_F gets closer to the top of the valence band with increasing [B] [Fig. 2(a)]. As a consequence, it also approaches the B energy level E_A, leading to a partial inoccupation of these B levels (1) and therefore to a reduced fraction of ionized B atoms [Fig. 2(b)]. At concentrations above 5×10^{16} cm^{-3} the amount of unionized B atoms starts to exceed 3%. When B atoms are compensated with P, E_F is shifted toward the middle of the gap [Fig. 2(a)] and moves away from E_A. This causes the fraction of ionized B to increase up to almost 100% as the compensation level $C_l = (N_A + N_D)/(N_A - N_D)$ increases from 1 to 1000 [Fig. 2(b)]. Surprisingly, this increase of the amount of ionized B atoms does not result in an increase of the i.i. ratio $p_0/(N_A\text{-}N_D)$ which remains nearly constant in the case of low [B] and slightly decreases with compensation for high [B] [Fig. 2(c)]. This is so because, as compensation increases, the net doping becomes smaller compared to [B] and thus a small amount of unionized B leads to a relatively strong effect on the carrier density. This observation shows that in compensated Si containing [B] $> 5 \times 10^{16}$ cm^{-3} as can be the case of UMG-Si, i.i. has to be taken into account to estimate p_0, no matter what the net doping is and even if the latter would be low enough to consider full ionization in the case of uncompensated Si.

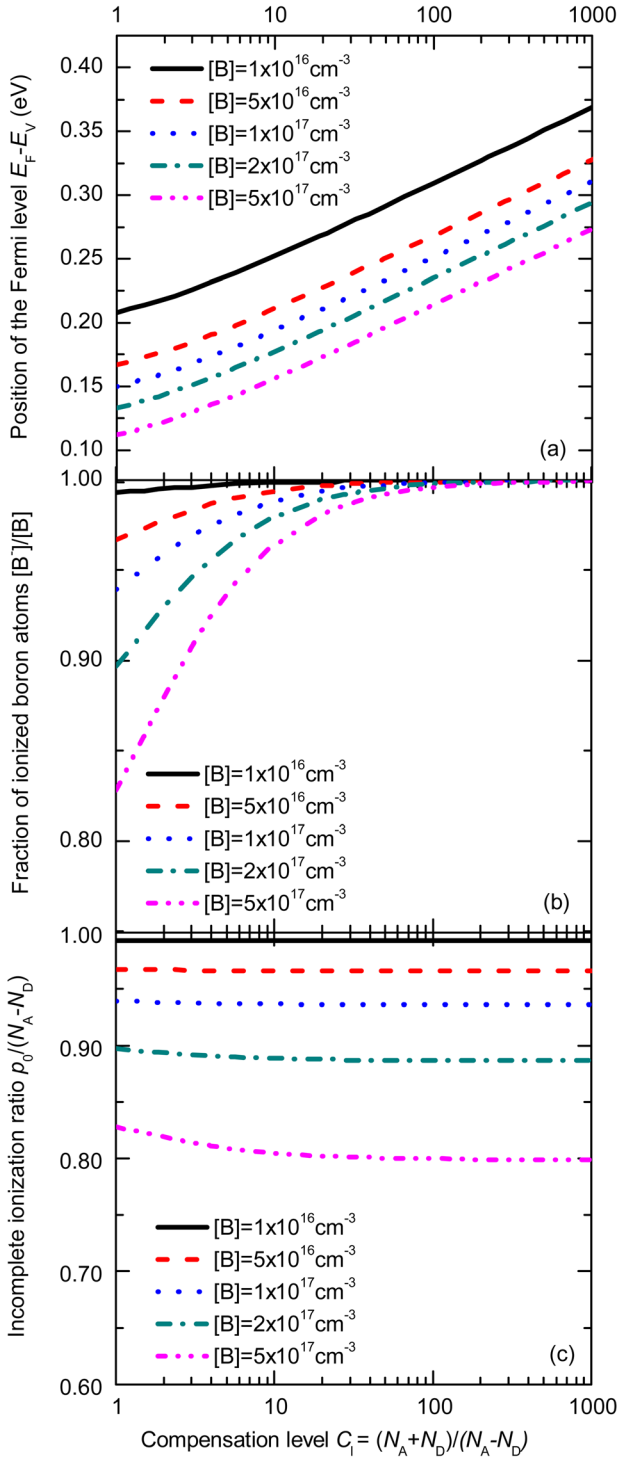

FIG. 2. (Color online) Calculation of the evolution of (a) the position of the Fermi level, (b) the fraction of ionized boron atoms and (c) the incomplete ionization ratio $p_0/(N_A\text{-}N_D)$ with the compensation level at 300 K in B and P co-doped Si.

Figure 3 shows the calculated i.i. ratio at 300 K as a function of the total concentration of acceptors in uncompensated Si and in highly phosphorus-compensated Si ($C_l = 1000$).

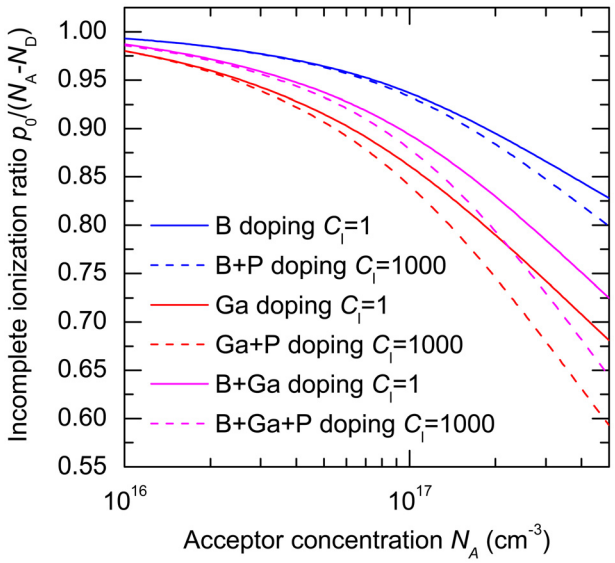

FIG. 3. (Color online) Dependence of the i.i. ratio with acceptor concentration in the case of B doping, Ga doping or a mixed doping of 50% of each. The i.i. ratio is represented for the cases of uncompensated Si (solid lines) and in the case of highly compensated Si with P (dashed lines).

Calculations are displayed for the cases of acceptors being B, Ga, or 50% of each. This plot summarizes well the three factors that affect i.i.:

(1) The total concentration of acceptors: in the relevant range of bulk doping for photovoltaic applications, i.i. increases with the total concentration of acceptors.
(2) The nature of acceptor dopants: as can be seen, i.i. increases with the fraction of gallium atoms among acceptor dopants due to their higher energy level in the bandgap.
(3) The compensation level: Fig. 3 shows that i.i. is systematically stronger in compensated Si and that the difference between compensated and uncompensated Si increases with the total density of acceptors.

2. Dependence on temperature

Figure 4(a) shows the T-dependence of the measured carrier density p_0 between 80 and 350 K on sample B-1 (B-doped), C-1 (co-doped with B, P, and Ga) and G-1 (Ga-doped). As can be seen, the carrier density is more strongly affected by i.i. at low temperature in the co-doped Si (decreased by more than three orders of magnitude at 80 K) than in uncompensated B- or Ga-doped Si of similar net doping (reduced at 80 K by a factor of 5 and 20, respectively). In uncompensated B-doped and Ga-doped samples, the carrier density is measured to be nearly constant near 300 K [see zoom in Fig. 4(b)] with an increase of about 0.7% in the B-doped sample and 2.4% in the Ga-doped sample between 300 and 350 K. This shows that both B- and Ga-doped samples are in the saturation range at 300 K, i.e., practically all dopants are ionized. On the contrary, p_0 keeps increasing by 15% between 300 and 350 K in the sample co-doped with B, P, and Ga. This demonstrates that, in this sample, the saturation range is not yet reached at 300 K and that acceptors are therefore not completely ionized. This confirms theoretical results presented in Sec. III A 1 showing that

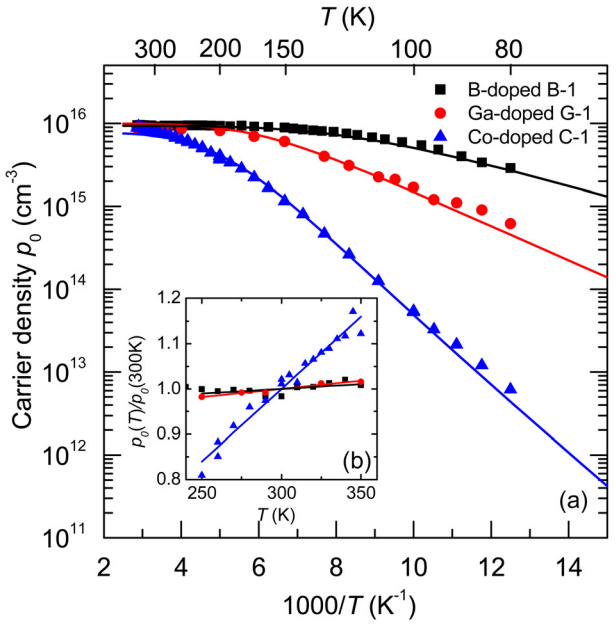

FIG. 4. (Color online) (a) T-dependence of the measured p_0 in B-doped Si (B-1), Ga-doped Si (G-1), and B, P, and Ga co-doped Si (C-1) of equivalent N_A-N_D. p_0 represented for sample G-1 is calculated from p_H data from Ref. 23. Solid lines represent p_0 as calculated using the method described in II. (b) Relative variation of p_0 in samples B-1, G-1, and C-1 around room-T. Solid lines are linear fits to the measured $p_0(T)/p_0(300\ \mathrm{K})$.

room-T i.i. is of greater importance in compensated Si than in uncompensated Si of same net doping. In the co-doped sample shown here, the high degree of i.i. can be explained by the three factors influencing i.i. mentioned before, i.e. the high acceptor density ($N_A = 8.0 \times 10^{16}$ cm^{-3}), the large fraction of Ga atoms among acceptors (72%) and the high compensation level ($C_I = 19$). For sample B-1 and C-1, T-dependences of the measured p_0 can be very well fitted with the carrier density calculated using the method described in Sec. II A. In sample G-1, the calculation agrees well with experimental data for a Ga concentration of 1.0×10^{16} cm^{-3} instead of the 1.5×10^{16} cm^{-3} given in Ref. 23. The good agreement between experimental data and calculations indicates that the parameterization of E_A in Table I is fairly accurate and that the potential influence of compensation on this parameter might be disregarded for the dopant concentrations considered in this work.

B. Incomplete ionization and carrier mobility

1. Comparison between experimental data and mobility model

The majority-carrier mobility in Si is known to be limited mostly by lattice-scattering (interaction with phonons) and by ionized impurity-scattering (Coulombic interaction with fixed charges). It is generally accepted that neutral impurity-scattering has only a very small, practically negligible impact on the overall mobility. Thus, only the concentration of ionized dopants should be used as an input in mobility models. Incomplete ionization of dopants is therefore to be accounted for when calculating the carrier mobility, especially at low T. Figure 5 shows the evolution of the

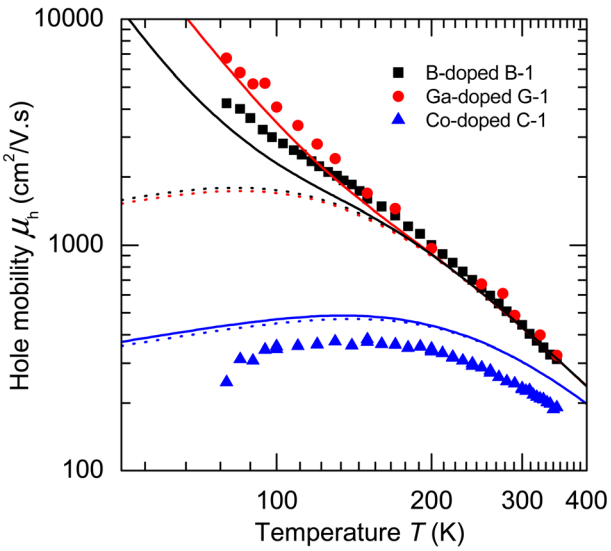

FIG. 5. (Color online) T-dependence of the measured hole mobility measured on samples B-1, G-1 and C-1. μ_h represented for sample G-1 is calculated from Hall mobility data from Ref. 23. The mobility calculated with Klaassen's model is represented by solid lines (incomplete ionization) and dotted lines (complete ionization).

majority-carrier mobility μ_h with T in samples B-1, C-1, and G-1 as deduced from the measured ρ and p_0 using the equation

$$\mu_h = \frac{1}{p_0 \cdot \rho \cdot q}. \quad (8)$$

Figure 5 also displays for each sample the carrier mobility as calculated with Klaassen's model[24,25] using either the total dopant densities (dashed lines) or the calculated ionized dopant concentrations (solid lines) as input parameters. In uncompensated B- and Ga-doped Si (B-1 and G-1), the experimental μ_h shows a perfect agreement with Klaassen's model around room-T. At lower T, experimental data agrees relatively well with the model when accounting for i.i. while it shows significant discrepancy if i.i. is neglected. It is worth noting that μ_h is measured to be the same in Ga-doped Si as in B-doped Si over the almost entire T range. This shows that ionized Ga atoms act as equivalent scattering centers to ionized B atoms. The only difference between μ_h in Ga- and in B-doped Si appears below 150 K, where i.i. starts to be important in Ga-doped Si, B-doped Si being still in the saturation range (Fig. 4). Although Klaassen's model has been developed for B-doped Si, it reproduces with equal accuracy μ_h in Ga-doped Si if i.i. of dopants is accounted for. It is therefore not necessary to distinguish between the two impurities when modeling μ_h in Si co-doped with B and Ga and the sum of both ionized concentrations can be used as a single input for the ionized acceptor density in Klaassen's model.

On the other hand, the mobility measured in co-doped sample C-1 is lower than the calculated mobility over the entire T range. Discrepancy between experimental and modeled mobility in compensated Si was already observed at room-T by several authors[10,12,13,15,26] who confronted their results to different models.[25,27–29] The deviation to the model was shown to increase with the compensation level.[13,15,30] It has been argued that the observed mobility reduction could be due to the existence of a compensation-specific scattering mechanism which standard mobility models do not take into account.[13,15] The following section will put this proposition to the test and show that it is not consistent with the T-dependence of the measured carrier mobility in compensated Si.

2. Impact of compensation on the carrier mobility

In compensated p-type Si, for which the total acceptor concentration is higher than the total donor concentration, the only possible E_F solution to the Poisson equation is located in the lower half of the bandgap. As a result, regardless of the temperature, P atoms are always completely ionized ($[P^+] = [P]$) and the concentration of ionized acceptor dopants cannot decrease below their concentration ($N_A^- > [P]$) but can only approach it as T reduces. Consequently, the total density of ionized dopants cannot decrease below $2 \times [P]$. This means that in highly compensated Si, in which the concentration of acceptor dopants is only slightly above [P], the density of ionized impurities will remain almost unchanged with decreasing T. For example, in co-doped sample C-1 studied in this work, the minimum value for the total concentration of ionized dopants is 14.2×10^{16} cm^{-3} which is very close (94.7%) to the total dopant concentration 15.0×10^{16} cm^{-3}. This fact is evidenced in Fig. 6 in which the calculated concentration of ionized dopant appears to be almost constant with T. This has three consequences:

(1) First, it implies that in highly compensated Si, incomplete ionization has only a weak influence on the dopant concentration used as input when calculating the carrier mobility. Since each ionized dopant densities remain almost constant with T, the modeled mobility is essentially the same whether taking i.i. into account or not, even at low T (Fig. 5).
(2) Second, ionized impurity-scattering is known to be more important at low T due to the increasing collision cross-section of fixed charges whereas lattice-scattering is dominant at high T because of stronger phonons. In

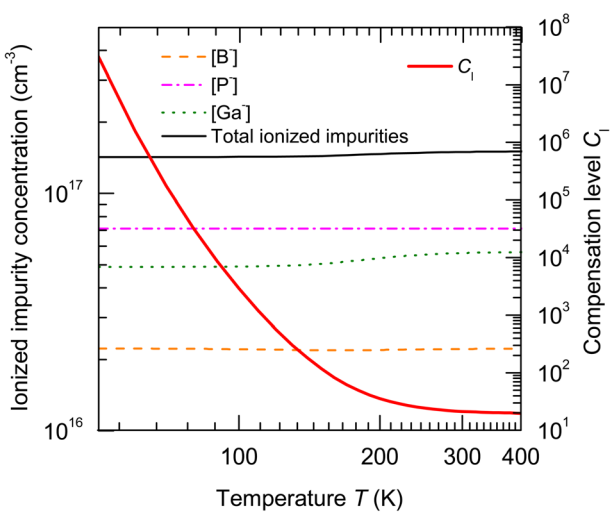

FIG. 6. (Color online) T-dependence of the calculated concentrations of ionized dopants and compensation level C_I in co-doped sampe C-1.

uncompensated Si, the increasing collision cross-section of ionized impurities is counterbalanced by the reduction of their concentration and therefore μ_h remains limited by lattice-scattering over the entire T range studied (keeps up increasing with decreasing T). In compensated Si, however, since the concentration of ionized impurities remains constant with reducing T while their collision cross-section simultaneously increases, μ_h becomes dominated by ionized impurity-scattering at low T, up to a relatively high T (140−150 K in sample C-1), at which it reaches its maximum (Fig. 5). As a consequence, μ_h varies with T within a much narrower range in compensated Si than in uncompensated Si.

(3) Lastly, since decreasing T leads to a reduction of p_0 by several orders of magnitude but keeps the total concentration of ionized dopants almost unchanged, it is equivalent to strongly increasing the compensation level C_1 Eq. (7). As can be seen on Fig. 6, the calculated C_1 in sample C-1 varies from 21 at 300 K to 3×10^4 at 80 K, which is far higher than any compensation level that has been reached in previous measurements conducted at room T. No μ_h drop is, however, observed at these low T which strongly challenges the potential existence of a compensation-specific scattering mechanism.

Previously,[13] μ_h has been measured to decrease by a factor of 5 below the theoretically expected value at a compensation level $C_1 = 140$. In the present work, the measured μ_h is lower than the mobility given by Klaassen's model but decrease only to about 75% of its value even at C_1 far above 140. The discrepancy between our results and those published by Veirman *et al*. might arise from the different ways compensation was achieved.

In the work by Veirman *et al*.,[13] compensation was tuned by activating oxygen-related thermal donors (TDs). Therefore, the carrier density uniformity depends strongly on the spatial distribution of oxygen and other point defects affecting TDs formation, which is known to be inhomogeneous.[31,32] As argued in a later paper,[33] p_0 heterogeneities could therefore be amplified when increasing compensation by TDs activation and might reduce μ_h if occurring on a microscopic scale or affect the validity of Hall effect measurements if occurring on a macroscopic scale. In the present work however, the studied sample is compensated because of the simultaneous presence of B, P, and Ga introduced during crystallization. Similar p_0 spatial non uniformities may exist in such material, depending on the crystallization process and the method used to introduce dopants. These would, however, not be amplified when compensation is increased by reducing T. If the lower μ_h measured in compensated Si is to be attributed to these heterogeneities, the underlying mechanism cannot therefore be designated as compensation-specific. Indeed, carrier density spatial non uniformities are not specific to compensated Si and are enhanced by compensation only under certain conditions.

Another hypothesis that has been formulated to explain the reduction of μ_h in compensated Si attributes it to a reduction of the screening of ionized impurities by free carriers[14,33,34] due to their lower concentration. Although such screening is taken into account by Klaassen's model, its impact on the collision cross-section could be underestimated. Indeed, Klaassen's model was parameterized to fit μ_h data in uncompensated Si in which ionized impurities and screening free carriers are present in equal concentration. Such an underestimation of the screening would lead to an underestimation of the scattering strength of ionized impurities by the model and therefore to an overestimation of the mobility in compensated Si. If this was the case, the discrepancy between measured data in compensated Si and Klaassen's model would be expected to increase at low T at which ionized impurity-scattering dominates. In sample C-1, however, measured and modeled mobility T-dependencies have the same shape. The measured mobility is reduced independently of T to about 75% of Klaassen's model. This indicates that the reduction of screening by free carriers is not alone sufficient to explain the reduction of carrier mobility in compensated Si.

To summarize this section, the T-dependence of the measured carrier mobility in compensated Si shows that its reduction compared to Klaassen's model cannot be explained by only the reduction of screening of ionized impurities by free carriers. Instead, the existence of p_0 heterogeneities, which can be amplified by compensation under certain conditions and remain invariable with T, could be a plausible explanation for the observed T-independent μ_h reduction. These heterogeneities are material-specific and should not be designated as compensation-specific.

C. Incomplete ionization and resistivity

For wafer control, resistivity measurement is commonly used to monitor the doping of Si. Although resistivity measurement does not allow the determination of dopant concentrations in compensated Si, it is very simple to implement in practice and can still be used to define material specifications in wafer and cell production. Since a larger carrier density variation with T appears around 300 K in compensated Si than in uncompensated Si, one could also expect the resistivity to be more variable for compensated Si in this T range. On the contrary, T-dependent resistivity measurements show the opposite behavior [Fig. 7(a) and 7(b)]. In uncompensated B- or Ga-doped Si, the majority-carrier mobility increases strongly with decreasing T near 300 K (Fig. 5), due to the reduction of phonon scattering. This leads, since the carrier density remains almost constant, to a reduction of the resistivity with decreasing temperature (Fig. 4). Below a certain temperature that depends on the impurity (∼100 K for B and ∼150 K for Ga), the freeze-out range is entered and, as the carrier density drops, the resistivity starts to increase again. In highly-doped compensated Si, the rise in majority-carrier mobility (Fig. 5) with decreasing temperature is weaker because the reduction of phonon scattering is counterbalanced by a stronger ionized-impurity scattering, as discussed in Sec. IV B. This moderate mobility increase, combined with the slow decrease of p_0 due to i.i., leads to an almost constant resistivity in the 250 to 350 K T range [Fig. 7(b)]. At temperatures below 200 K, the carrier density falls sharply and the resistivity is drastically increased by several orders of magnitude. The fact that the resistivity stays nearly

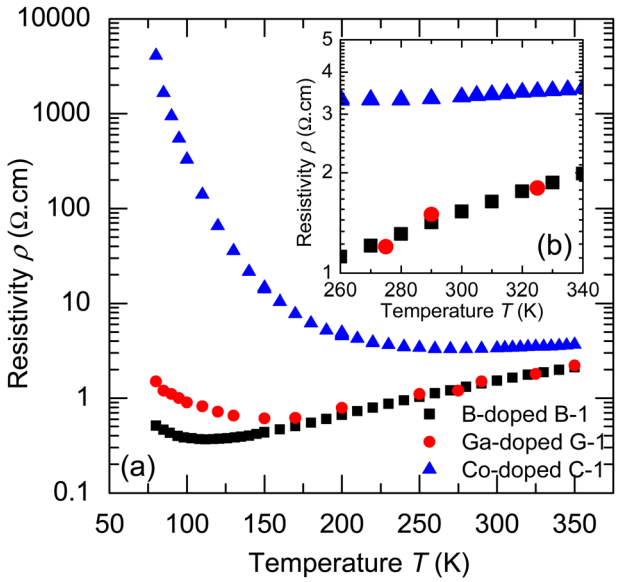

FIG. 7. (Color online) (a) T-dependence of the resistivity in samples B-1, G-1, and C-1. (b) Zoom on the resistivity around room-T.

constant around room-T in compensated Si means that T stability during wafer control is not as critical as in the case of uncompensated Si.

IV. CONCLUSION

In summary, both calculations and Hall-effect measurements show that incomplete ionization is of greater importance in highly doped compensated Si than in uncompensated Si of the same net doping. Room-temperature incomplete ionization should be taken into account when evaluating p_0 whenever [B] is higher than 5×10^{16} cm^{-3} or [Ga] higher than 2×10^{16} cm^{-3}, regardless of the net dopant density.

Calculations also show that the compensation level can be tuned by reducing the temperature. Since no majority-carrier mobility drop is measured to occur at low temperature where the compensation reaches extreme values, the existence of a compensation-specific scattering mechanism is very unlikely. It is shown that the reduction of ionized impurity screening by free carriers cannot alone explain the reduction of majority-carrier mobility in compensated Si compared to Klaassen's model, over the entire 80−350 K temperature range. On the contrary, carrier density spatial heterogeneities, which could increase with the concentration of compensating donors and are unaffected by temperature variations, might explain the reduction in majority-carrier mobility over the entire temperature range.

Although carrier density variations with temperature are greater in compensated Si due to stronger i.i., they do not lead to stronger variations of the resistivity near room-temperature. The resistivity is actually more stable in highly doped compensated Si around room-T than in uncompensated Si, due to the weaker dependence of majority-carrier mobility on T.

[1]J. Kraiem, B. Drevet, F. Cocco, N. Enjalbert, S. Dubois, D. Camel, D. Grosset-Bourbange, D. Pelletier, T. Margaria, and R. Einhaus, in *Proceedings 35th IEEE Photovoltaic Specialists Conference*, Hawaii (IEEE, New York, 2010).
[2]S. Dubois, N. Enjalbert, and J. P. Garandet, Appl. Phys. Lett. **93**, 032114 (2008).
[3]D. Macdonald and A. Cuevas, J. Appl. Phys. **109**, 043704 (2011).
[4]S. Pizzini and C. Calligarich, J. Electrochem. Soc. **131**, 2128 (1984).
[5]J. Kraiem, R. Einhaus, and H. Lauvray, in *Proceedings 34th IEEE Photovoltaic Specialists Conference*, Philadelphia (IEEE, New York, 2009), p. 1327.
[6]D. Macdonald, F. Rougieux, A. Cuevas, B. Lim, J. Schmidt, M. D. Sabatino, and L. J. Geerligs, J. Appl. Phys. **105**, 093704 (2009).
[7]J. Veirman, S. Dubois, N. Enjalbert, J. P. Garandet, and M. Lemiti, J. Appl. Phys. **109**, 103711 (2011).
[8]J. Geilker, W. Kwapil, and S. Rein, J. Appl. Phys. **109**, 053718 (2011).
[9]C. Modanese, M. Di Sabatino, A.-K. Soiland, K. Peter, and L. Arnberg, Progr. Photovoltaics **19**, 45 (2010).
[10]F. E. Rougieux, D. Macdonald, A. Cuevas, S. Ruffell, J. Schmidt, B. Lim, and A. P. Knights, J. Appl. Phys. **108**, 013706 (2010).
[11]B. Lim, V. V. Voronkov, R. Falster, K. Bothe, and J. Schmidt, Appl. Phys. Lett. **98**, 162104 (2011).
[12]M. Forster, E. Fourmond, R. Einhaus, H. Lauvray, J. Kraiem, and M. Lemiti, Phys. Status Solidi C **8**, 678 (2011).
[13]J. Veirman, S. Dubois, N. Enjalbert, J. P. Garandet, D. R. Heslinga, and M. Lemiti, Solid-State Electron. **54**, 671 (2010).
[14]B. Lim, M. Wolf, and J. Schmidt, Phys. Status Solidi C **8**, 835 (2011).
[15]E. Fourmond, M. Forster, R. Einhaus, H. Lauvray, J. Kraiem, and M. Lemiti, Energy Procedia **8**, 349 (2011).
[16]S. M. Sze and K. K. Ng, *Physics of Semiconductor Devices* (Wiley Interscience, New York, 2007).
[17]M. A. Green, J. Appl. Phys. **67**, 2944 (1990).
[18]P. P. Altermatt, A. Schenk, and G. Heiser, J. Appl. Phys. **100**, 113714 (2006).
[19]P. P. Altermatt, A. Schenk, B. Schmithusen, and G. Heiser, J. Appl. Phys. **100**, 113715 (2006).
[20]K. B. Wolfstirn, J. Phys. Chem. Solids **16**, 279 (1960).
[21]D. W. Fischer and J. J. Rome, Phys. Rev. B **27**, 4826 (1983).
[22]F. Szmulowicz, Phys. Rev. B **34**, 4031 (1986).
[23]T. Hoshikawa, T. Taishi, K. Hoshikawa, I. Yonenaga, and S. Uda, Jpn. J. Appl. Phys. **48**, 031102 (2009).
[24]D. B. M. Klaassen, Solid-State Electron. **35**, 953 (1992).
[25]D. B. M. Klaassen, Solid-State Electron. **35**, 961 (1992).
[26]F. E. Rougieux, D. Macdonald, and A. Cuevas, Progress in Photovoltaics: Research and Applications **19**, 787 (2011).
[27]N. D. Arora, J. R. Hauser, and D. J. Roulston, IEEE Trans. Electron Devices **29**, 292 (1982).
[28]S. Reggiani, M. Valdinoci, L. Colalongo, M. Rudan, G. Baccarani, A. D. Stricker, F. Illien, N. Felber, W. Fichtner, and L. Zullino, IEEE Trans. Electron Devices **49**, 490 (2002).
[29]J. M. Dorkel and P. Leturcq, Solid-State Electron. **24**, 821 (1981).
[30]A. Cuevas, M. Forster, F. Rougieux, and D. Macdonald, Energy Procedia (in press).
[31]A. Murgai, H. C. Gatos, and W. A. Westdorp, J. Electrochem. Soc. **126**, 2240 (1979).
[32]W. V. Ammon, P. Dreier, W. Hensel, U. Lambert, and L. Koster, Mater. Sci. Eng., B **36**, 33 (1996).
[33]J. Veirman, S. Dubois, N. Enjalbert, J. P. Garandet, D. R. Heslinga, and M. Lemiti, Phys. Status Solidi C **8**, 729 (2011).
[34]B. Lim, F. Rougieux, D. Macdonald, K. Bothe, and J. Schmidt, J. Appl. Phys. **108**, 103722 (2010).